ACS OMEGA

Open Access

http://pubs.acs.org/journal/acsodf

Article

Oxidation and Hydrolysis of Ginsenoside Rg5: An Underestimated Degradation Pathway, Isolation, and Characterization of Unknown Degradation Products

Leqin Cheng,* Anqi Ye, Yunqi Tao, and Yuewei Zhang*

Cite This: *ACS Omega* 2025, 10, 15732−15743

Read Online

ACCESS | Metrics & More | Article Recommendations | Supporting Information

ABSTRACT: Ginsenoside Rg5, a secondary ginsenoside derived from the degradation of protopanaxadiol saponins, exhibits various pharmacological activities, including anticancer, anti-inflammatory, antidiabetic, and memory-enhancing effects, making it a promising candidate for natural medicine. However, research on the stability of Rg5, particularly in aqueous solutions, remains limited. This study systematically investigates the stability of ginsenoside Rg5 in water by monitoring its degradation over time under controlled conditions. The stability of the Rg5 aqueous solution was assessed by investigating the influences of temperature and time, employing high-performance liquid chromatography (HPLC) analysis to evaluate its degradation. The findings indicated substantial degradation of Rg5, with approximately 95% decomposition observed after a period of 10 days. The decomposition products were isolated using preparative liquid chromatography and identified through high-resolution mass spectrometry (HR-MS), NMR, and induced circular dichroism (ICD) analyses. A novel derivative was identified, and its degradation pathway was elucidated, encompassing oxidation, hydrolysis, and dehydration processes that culminated in the formation of four distinct stereoisomers. This study elucidates the instability of Rg5 in aqueous environments and offers significant insights into its decomposition mechanism. The findings emphasize the critical importance of optimizing storage conditions and minimizing exposure to water and oxygen to enhance the stability of Rg5, thereby advancing its potential applications in pharmaceutical development and storage.

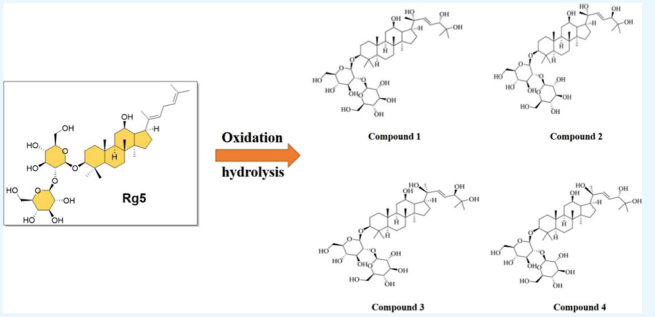

INTRODUCTION

Ginseng saponin is an important active ingredient in the plant genus *Panax ginseng*. According to its structure, ginseng saponin is mainly divided into protopanaxadiol saponin (PPD saponin, including ginsenoside Ra1, Ra2, Ra3, Rb1, Rb2, Rb3, Rc, Rd, etc.), protopanaxatriol saponin (PPT saponin, including Rg1, Re, Rf, etc.), and oleanolic acid-type saponins (Ro). Among them, protopanaxadiol saponin and protopanaxatriol saponin belong to tetracyclic triterpenoid saponins, while the oleanolic acid-type saponins belong to pentacyclic triterpenoid saponins. Many original ginseng saponins contained in ginseng are difficult to be absorbed by the human body. For example, most of them in Rb1, Rb2, Rb3, and Rc are excreted from the body, so their bioavailability is very low.[1,2] Rare ginsenosides are secondary metabolites derived from the metabolic transformation of major ginsenosides, such as Rb1, Rc, Rb2, Rd, Re, and Rg1, within plants. Additionally, they can be produced in vitro through processes like hydrolysis, enzymatic hydrolysis, and microbial transformation of these major ginsenosides. Examples of rare ginsenosides include compound K, F4, Rg3, Rg5, Rg6, Rh1, Rh2, Rh3, Rh4, Rk1, Rk2, Rk3, aPPD, and aPPT, among others. Numerous studies have demonstrated that rare ginsenosides exhibit enhanced ability to traverse the intestinal barrier and enter the circulatory system, thereby substantially increasing the bioavailability of ginsenosides. For instance, when administered orally, hydrophilic major ginsenosides undergo metabolic conversion into low-polarity, hydrophobic rare ginsenosides such as compound K, Rh1, and Rh2, which are subsequently absorbed into the bloodstream.[3] Furthermore, rare ginsenosides demonstrate enhanced anticancer properties.[4,5] Park et al.[6] conducted a comparative study examining the inhibition of AGS cell proliferation through the application of the major ginsenosides Rb1 and Re as well as their respective degradation products. The degradation product of Rb1 was characterized by a substantial presence of rare ginsenosides, including 20(*S*,*R*)-Rg3, Rk1, and Rg5, while the degradation product of Re contained significant amounts of rare ginsenosides Rg2, Rg6, and F4. The findings

Received: February 15, 2025
Revised: March 14, 2025
Accepted: April 3, 2025
Published: April 9, 2025

https://doi.org/10.1021/acsomega.5c01444
ACS Omega 2025, 10, 15732−15743

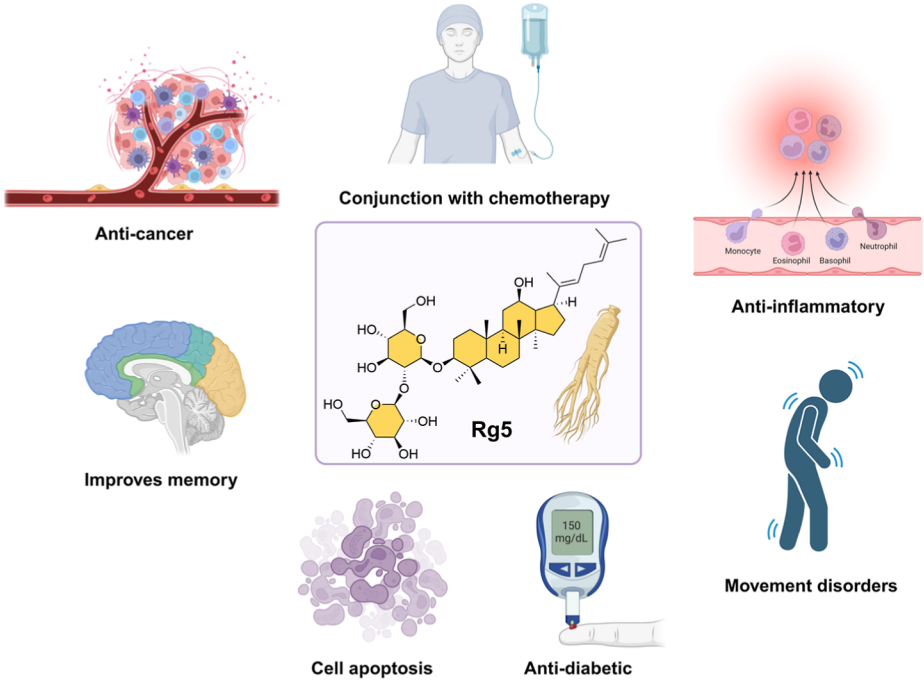

Figure 1. Different biological and pharmacological properties of Rg5.

from the experiment indicated that neither Rb1 nor Re alone was effective in inhibiting AGS cell proliferation. However, their degradation products demonstrated notable anticancer activity, with the degradation product of Rb1 exhibiting a particularly significant inhibitory effect on AGS cell proliferation. The rare ginsenoside Rg5, a degradation product of protopanaxadiol saponins, was initially isolated from red ginseng by a South Korean research team.[7] Currently, ginsenoside Rg5 is predominantly obtained from heat-processed ginseng,[8,9] directly extracted from ginseng powder while degrading ginsenosides,[10] derived from ginseng roots, stems, and leaves extracts,[11] prepared from PPD saponins,[12] or prepared from ginsenoside Rb1.[13,14] Research on the pharmacological properties of ginsenoside Rg5 has demonstrated its significant anticancer efficacy[15−17] (Figure 1). Furthermore, when administered in conjunction with chemotherapy agents, such as docetaxel (TXT), Rg5 has been shown to mitigate drug resistance without exacerbating toxicity.[18] For instance, Liu and Fan[15] performed cytotoxic assays on a range of human cancer cell lines, including MCF-7, CACO-2, SGC-7901, NCI-H460, and SMMC-7721, utilizing ginsenosides Rb1, R-Rg3, S-Rg3, and Rg5. The findings indicated that ginsenoside Rg5 demonstrated the greatest cytotoxicity across the various cancer cell lines. Kim et al.[8] conducted cytotoxic experiments on MCF-7 and MDA-MB-453 breast cancer cell lines using ginsenoside Rg5 and 20S-Rg3. The results showed that ginsenoside Rg5 exhibited more significant cytotoxicity than 20S-Rg3. Feng et al.[18] demonstrated that the combination of ginsenoside Rg5 with docetaxel (TXT) significantly inhibits the growth of drug-resistant tumors without exacerbating toxicity relative to TXT monotherapy. This finding suggests that ginsenoside Rg5 effectively enhances the response to tumor resistance. Ginsenoside Rg5 also exhibits antidiabetic[19] and anti-inflammatory activities[20] and improves memory function.[21] In addition, Panossian et al.[22] studied the effect of Rg5 on the expression of the HT22 gene in mouse neuronal cells from a genetic perspective. The findings of the study indicate that Rg5 exhibits modest yet advantageous effects on apoptosis, movement disorders, and cancer, suggesting its potential application as a natural therapeutic agent.

The majority of naturally occurring active organic molecules isolated from living organisms are susceptible to decomposition when exposed to natural environments. The stability of these active molecules significantly influences their pharmacological properties and potential adverse reactions. Furthermore, stability is a critical consideration in determining appropriate packaging, storage, transportation methods, and shelf life. Currently, numerous studies investigate the pharmacological activities of ginsenosides; however, research on their stability remains limited, with the primary focus being the influence of temperature as a determining factor. Kim et al.[23] studied the effect of temperature between 100 and 120 °C on ginsenosides. Raw ginseng samples were exposed to steaming in autoclaves at temperatures of 100, 110, and 120 °C for a period of 2 h. The findings demonstrated that as the steaming temperature increased, there was a significant decrease in the concentrations of the major ginsenosides Rb1, Rb2, Rc, Rd, Re, and Rg1. In contrast, there was a marked increase in the levels of the rare ginsenosides Rg3, Rg5, and F4. This indicates that the major ginsenosides Rb1, Rb2, Rc, Rd, Re, and Rg1 have poor stability under conditions of 100−120 °C, and most of them degrade into rare ginsenosides. Song et al.[24] prepared ginseng decoction pieces from fresh ginseng slices using methods of blast drying (40−80 °C), shade drying, sun drying, microwave drying, and freeze-drying and investigated the changes in the ginsenoside content. The experimental results show that the order of total saponin content from high to low is freeze-drying > shade drying > blast drying at 40 °C > blast drying at 50 °C > sun drying > drying of 80 °C > blast drying at 60 °C > blast drying at 70 °C, which also indicates that relative low temperature is beneficial for saponin stability. Zhu et al.[25] studied the effects of high temperature, humidity, and light on the stability of ginsenoside CK hydrate. The results showed that the hemihydrate,

https://doi.org/10.1021/acsomega.5c01444
ACS Omega 2025, 10, 15732−15743

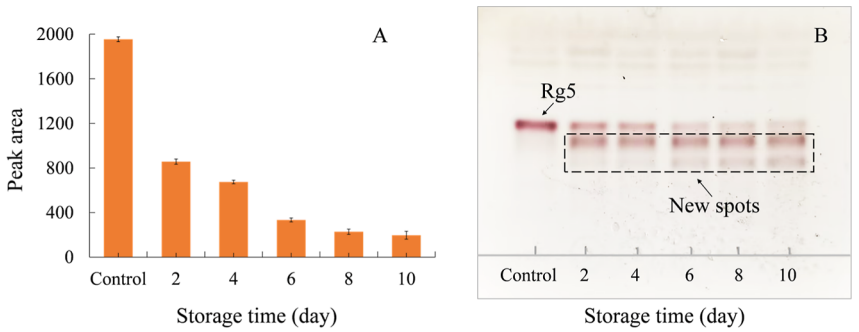

Figure 2. Analysis of time-course decomposition of ginsenoside Rg5 in aqueous solvent. (A) Analysis of peak area of ginsenoside Rg5 in aqueous solvent. (B) TLC analysis of decomposition products of ginsenoside Rg5 in aqueous solvent.

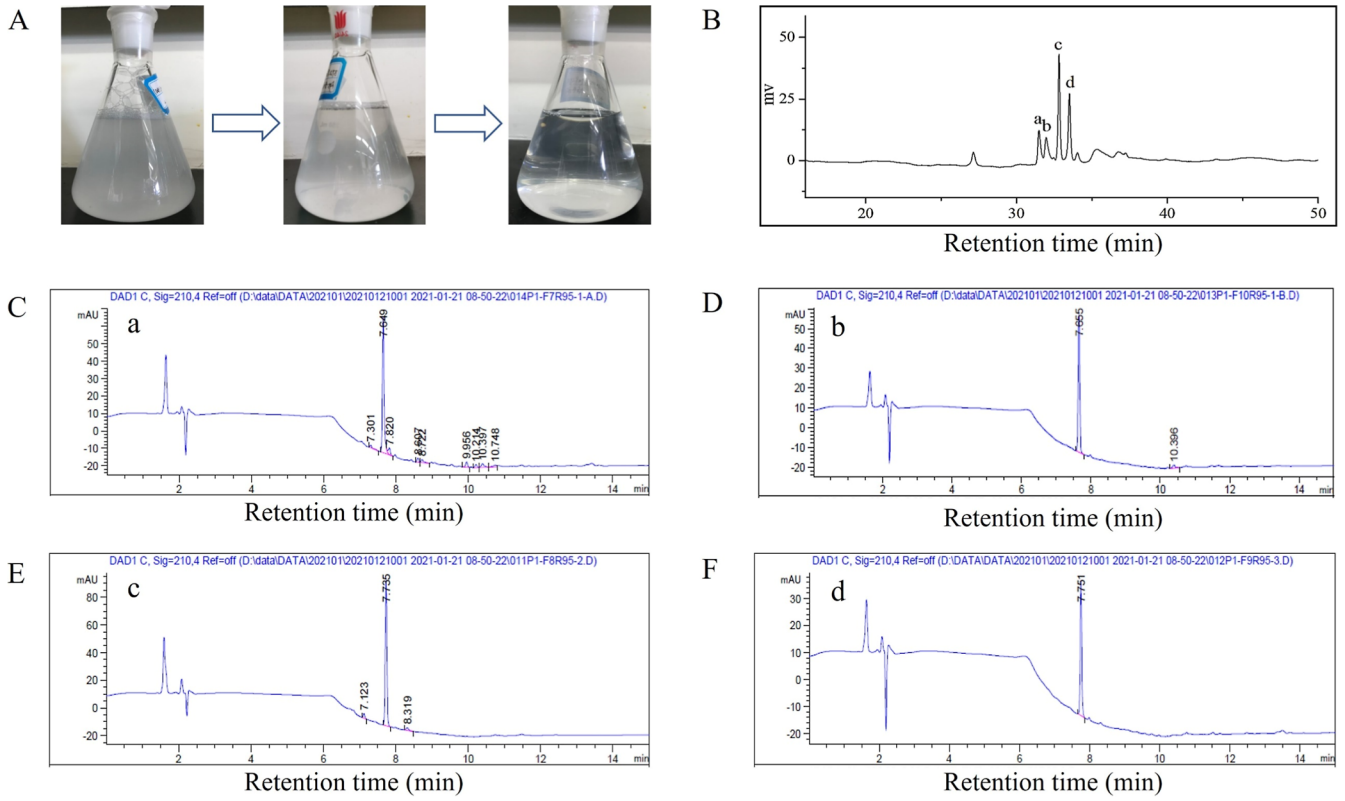

Figure 3. Decomposition process of ginsenoside Rg5 in water and the HPLC analysis of the decomposition products. (A) Decomposition process diagram of ginsenoside Rg5 in water; (B) HPLC analysis of the decomposition products of ginsenoside Rg5 in water (HPLC analysis adopts the first method); (C−F) HPLC analysis of the decomposition products a−d of ginsenoside Rg5 in water (HPLC analysis adopts the second method).

monohydrate, and dihydrate of ginsenoside CK were stable under high humidity (relative humidity of 75% for 10 days) and light (light intensity of 3500 Lx for 10 days) conditions, while the hemihydrate and monohydrate were stable under high temperature (temperature of 80 °C for 10 days) conditions. However, commencing from the fifth day, a reduction in the moisture content of the dihydrate was observed. In addition, Chen et al.[11] studied the effects of light and temperature on the stability of ginsenoside Rg5 and found that ginsenoside Rg5 was unstable under light and 45 °C; especially after 30 days of light exposure, the amount of Rg5 significantly decreased.

The structural stability of compounds in natural environments is primarily influenced by factors such as temperature, humidity, light exposure, acidity, and alkalinity.[26−28] Comprehending the influence of environmental factors on the stability of bioactive compounds is essential for pharmaceutical research. Water is an unavoidable and important factor affecting the stability of drugs. Therefore, this article examines the impact of water on the stability of ginsenoside Rg5. Through the isolation and characterization of the primary decomposition products of Rg5 in aqueous environments, this study investigates the potential decomposition pathways of ginsenoside Rg5. The findings offer a theoretical foundation for the preparation, storage, transportation, and pharmaceutical application of ginsenoside Rg5.

RESULT AND DISCUSSION

An aqueous suspension of ginsenoside Rg5, at a concentration of 0.1 mg/mL, was subjected to agitation in a desktop shaker oscillator set at 25 °C and operated at 100 rpm for a duration of 2−10 days. Subsequently, an appropriate volume of anhydrous ethanol was added to the sample, followed by

https://doi.org/10.1021/acsomega.5c01444
ACS Omega 2025, 10, 15732−15743

rotary evaporation to achieve dryness. The resultant residue was then dissolved in HPLC-grade methanol and subjected to analysis via high-performance liquid chromatography (HPLC) to quantify the remaining Rg5 content. The findings from this analysis are presented in Figure 2A. The analysis of the peak area variations of ginsenoside Rg5 over different storage durations indicates a rapid decomposition rate of Rg5 in aqueous conditions. Specifically, after 2 days of storage, approximately 56% of ginsenoside Rg5 had undergone decomposition, with the decomposition rate escalating to 90% after 10 days. This proves that Rg5 is highly unstable in aqueous conditions. The results of the TLC analysis presented in Figure 2B demonstrate that with extended storage duration, the intensity of the Rg5 spots diminishes progressively. Concurrently, two distinct purple spots with higher polarity emerge below ginsenoside Rg5. This observation suggests that ginsenoside Rg5 undergoes decomposition into more polar saponins in aqueous conditions.

A total of 375 mg of ginsenoside Rg5 was incorporated into 500 mL of distilled water and agitated to produce a water suspension of ginsenoside Rg5 (refer to Figure 3A-1). The suspension was then placed in a desktop shaker oscillator maintained at 25 °C and oscillated for a duration of 10 days (see Figure 3A-2). Subsequently, the oscillation was continued in the desktop shaker oscillator at 45 °C to facilitate the decomposition process until the solution became completely clear (refer to Figure 3A-3). Figure 3 illustrates the progressive clarification of the aqueous solution of ginsenoside Rg5 from turbidity, suggesting that ginsenoside Rg5 undergoes structural modifications in water, resulting in its transformation into a more water-soluble decomposed saponin compared to Rg5. The decomposition product of ginsenoside Rg5 in water was subsequently concentrated and dissolved in HPLC-grade methanol for high-performance liquid chromatography (HPLC) analysis. As shown in Figure 3B, four new absorption peaks labeled as a−d appeared clearly during the retention time of 30−35 min. The decomposition products a (compound **1**), b (compound **2**), c (compound **3**), and d (compound **4**) were separated by preparative liquid chromatography (see Figure 3C−F) to obtain 14.33 mg, 13.75 mg, 24.80 mg, and 20.70 mg of monomers, respectively. At the same time, two compounds **5** (1.79 mg) and **6** (5.65 mg) were separated.

In order to clarify the structure of the decomposition products (compounds **1**−**4**) of ginsenoside Rg5 in water, HR-MS, ^{1}H NMR, ^{13}C NMR, HMBC (heteronuclear multiple, and HSQC (heteronuclear single quantum correlation) were performed (see Figures S1−S20) and characterized in combination with literature. The analysis results of ^{1}H NMR and ^{13}C NMR data for compounds **1**, **2**, **3**, and **4** are shown in Tables 1 and 2. Compound **1** is a white powder, and based on the $[M + Na]^+$ signal of m/z 839.47399 provided by HR-MS, its molecular formula is speculated to be $C_{42}H_{72}O_{15}$, with an degree of unsaturation of 7. Compared with ginsenoside Rg5 ($C_{42}H_{70}O_{12}$), compound **1** exhibits an increase of two hydrogen atoms and three oxygen atoms, accompanied by a reduction of one degree of unsaturation. The ^{1}H NMR analysis of compound **1** shows two coupled signals at δ_H 6.05 ppm (1H, d, J = 15.6 Hz) and δ_H 6.50 ppm (1H, dd, J = 6.6, 15.6 Hz), indicating the presence of two hydrogen atoms in compound **1** that are, respectively, connected to two double-bonded carbon atoms (=C−H), and the coupling constant (J) is 15.6 Hz, indicating that the double bond structure is E-configuration. The singlet signals appearing at δ_H 0.85, 0.94, 1.03, 1.13, 1.32, 1.56, 1.56, and 1.57 ppm belong to methyl hydrogens at positions 19, 30, 18, 29, 28, 21, 26, and 27. In addition, it also contains two signals for the anomeric proton of glucoses, namely, the inner proton appearing at δ_H 4.96 ppm (1H, d, J = 7.8 Hz, H-1′) and the outer proton appearing at δ_H 5.40 ppm (1H, d, J = 7.2 Hz, H-1″), indicating that compound **1** contains two β-D-glucopyranoses.

^{13}C NMR analysis shows that compound **1** has 42 carbon signals, corresponding to the carbon count of Rg5. Among these, 12 signals, as detailed in Table 2, are observed at chemical shifts of δ_C 105.16, 83.54, 78.38, 71.67, 78.29, 62.74

Table 1. ^{1}H NMR Data of Compounds 1−4 in Pyridine-d_5 (δ in ppm)

no.	compound **1**	compound **2**	compound **3**	compound **4**
1	0.77 m	0.77 m	0.76 m	0.77 m
	1.52 m	1.51 m	1.50 m	1.50 m
2	1.83 m	1.83 m	1.82 m	1.83 m
	2.22 m	2.20 m	2.20 m	2.19 m
3	3.31 dd (3.6, 11.4)	3.30 dd (4.2,11.4)	3.29 dd (4.2,11.4)	3.29 dd (4.2,11.4)
5	0.70 br d (11.4)	0.70 br d (11.4)	0.69 br d (11.4)	0.69 br d (11.4)
6	1.39 m	1.40 m	1.35 m	1.37 m
	1.51 m	1.51 m	1.48 m	1.48 m
7	1.23 m	1.22 m	1.22 m	1.21 m
	1.45 m	1.45 m	1.46 m	1.45 m
9	1.42 m	1.41 m	1.40 m	1.41 m
11	1.42 m	1.42 m	1.48 m	1.56 m
	2.06 m	2.06 m	2.00 m	1.93 m
12	3.93 m	3.93 m	3.92 m	3.93 m
13	2.02 m	2.02 m	2.00 m	2.03 m
15	1.01 m	1.01 m	1.04 m	1.04 m
	1.54 m	1.55 m	1.59 m	1.59 m
16	1.45 m	1.45 m	1.60 m	1.56 m
	1.90 m	1.88 m	1.94 m	1.93 m
17	2.42 m	2.40 m	2.41 m	2.41 m
18	1.03 s	1.03 s	1.01 s	1.02 s
19	0.85 s	0.85 s	0.79 s	0.81 s
21	1.56 s	1.56 s	1.56 s	1.58 s
22	6.41 d (15.6)	6.36 d (15.6)	6.42 d (15.0)	6.51 d (15.6)
23	6.50 dd (15.6, 6.6)	6.45 dd (15.6, 6.6)	6.54 dd (15.0, 7.2)	6.31 dd (15.6, 6.6)
24	4.47 d (5.4)	4.45 d (6.6)	4.48 d (7.2)	4.44 d (6.6)
26	1.56 s	1.56 s	1.61 s	1.58 s
27	1.57 s	1.56 s	1.62 s	1.60 s
28	1.32 s	1.32 s	1.30 s	1.30 s
29	1.13 s	1.13 s	1.10 s	1.10 s
30	0.94 s	0.93 s	0.97 s	0.97 s
1′	4.96 d (7.2)	4.96 d (7.8)	4.93 d (7.8)	4.94 d (7.8)
2′	4.25 m	4.26 m	4.24 m	4.24 m
3′	4.33 m	4.33 m	4.32 m	4.32 m
4′	4.16 m	4.16 m	4.16 m	4.16 m
5′	3.97 m	3.97 m	3.95 m	3.96 m
6′	4.49 m	4.50 m	4.49 m	4.49 m
1″	5.40 d (7.2)	5.40 d (7.2)	5.38 d (7.8)	5.38 d (7.8)
2″	4.15 m	4.15 m	4.14 m	4.14 m
3″	4.26 m	4.26 m	4.26 m	4.26 m
4″	4.36 m	4.37 m	4.36 m	4.36 m
5″	4.94 m	3.94 m	3.93 m	3.94 m
6″	4.36 m	4.36 m	4.35 m	4.36 m
	4.58 m	4.58 m	4.56 m	4.56 m

https://doi.org/10.1021/acsomega.5c01444
ACS Omega 2025, 10, 15732−15743

Table 2. ^{13}C NMR Data of Compounds 1−4 in Pyridine-d_5 (δ in ppm)

no.	compound 1	compound 2	compound 3	compound 4
1	39.20	39.20	39.18	39.20
2	26.78	26.77	26.76	26.77
3	88.95	88.97	88.96	88.97
4	39.74	39.74	39.71	39.72
5	56.43	56.44	56.41	56.41
6	18.48	18.48	18.46	18.46
7	35.21	35.22	35.22	35.23
8	40.04	40.04	39.96	39.99
9	50.38	50.38	50.41	50.43
10	36.96	36.97	36.92	36.93
11	32.11	32.12	32.28	32.26
12	70.76	70.77	71.01	70.99
13	49.76	49.75	50.24	50.14
14	51.78	51.83	51.92	51.95
15	31.51	31.53	31.54	31.51
16	27.30	27.38	26.51	26.57
17	52.33	52.10	53.75	53.69
18	15.82	15.82	15.93	15.90
19	16.44	16.44	16.39	16.42
20	73.48	73.53	74.00	74.05
21	21.66	21.54	29.30	28.82
22	140.64	141.05	136.40	136.16
23	128.25	128.30	130.40	130.29
24	79.80	80.03	79.98	80.07
25	72.81	72.71	72.79	72.74
26	26.62	26.77	26.70	27.0
27	25.82	25.72	25.71	25.62
28	28.15	28.16	28.14	28.13
29	16.63	16.64	16.60	16.60
30	17.27	17.29	17.39	17.37
1′	105.16	105.17	105.17	105.16
2′	83.54	83.54	83.52	83.52
3′	78.38	78.00	78.36	77.99
4′	71.67	71.67	71.65	71.66
5′	78.29	78.15	78.13	78.28
6′	62.74	62.75	62.73	62.73
1″	106.13	106.13	106.12	106.12
2″	77.20	77.20	77.20	77.20
3″	78.00	78.38	78.00	78.13
4″	71.70	71.70	71.70	71.69
5″	78.15	78.29	78.28	78.36
6″	62.89	62.90	62.88	62.88

ppm, and 106.13, 77.20, 78.00, 71.70, 78.15, and 62.89 ppm, which are indicative of two glucose moieties. Among them, δ_C 105.16 and δ_C 106.13 correspond to two anomeric carbon of glucose, respectively. Within the range of δ_C 110−150 ppm, only two signal peaks were observed at δ_C 141.64 and δ_C 128.25, indicating that compound **1** only contains one C═C double bond, which is one less double bond than Rg5. This observation further suggests that the decomposition of ginsenoside Rg5 in aqueous environments is associated with the presence of the double bond functional group. In the range of δ_C 70−90 ppm, in addition to the 10 carbon atoms belonging to glucose, five signal peaks of carbon atoms connected to hydroxyl groups can also be observed, which is three more than Rg5. Among them, the signal for C-3 appeared at δ_C 88.95 ppm, the signal for C-12 appeared at δ_C 70.76 ppm, and the other signals have not appeared in ginsenoside Rg5, indicating that three new hydroxyl groups are generated at the aliphatic chain connected of ginsenoside Rg5 after decomposition. The HMBC spectrum is a heteronuclear multicarbon correlation spectrum of ^1H, which associates the ^1H nucleus with the remote coupled ^{13}C nucleus. Typically, protons that are separated by two to three bonds generally exhibit stronger coupling interactions with carbon atoms. Consequently, information regarding carbon atoms located two to three bonds away from the proton can be effectively observed. To determine the specific position of the double bond on the aliphatic chain, HMBC analysis was performed on compound **1** (see Figure S13), and carbon related peaks were analyzed using H-17, which is easily recognizable in tetracyclic triterpenoid ginsenosides (see Figure 4A).

The signal of H-17 in the ^1H NMR analysis of compound **1** appeared at 2.43 ppm (see Figure 4A). As shown in Figure 4A, there is a correlation between the appearance of 17-H at δ_H 2.43 ppm and the carbon atoms at δ_C 21.69, 27.49, 49.68, 70.76, 73.37, and 140.63 ppm. The carbon atom at δ_C 140.63 ppm is a double bond carbon atom. Based on the fact that the double bond in compound **1** is an *E*-configuration, it can be inferred that the signal at δ_C 140.63 ppm belongs to 22-C, that is, the double bond carbon atoms in compound **1** are located at positions 22 and 23, while the carbon atoms corresponding to other chemical shifts are C-21 (21.69 ppm), C-16 (27.49 ppm), C-13 (49.68 ppm), C-12 (70.76 ppm), and C-20 (73.37 ppm), respectively (see Figure 4B). With the determination of double bond carbon atoms, the attribution of the three hydroxyl groups in the aliphatic chain can be further characterized. They are located at positions C-20, C-24, and C-25, respectively. Combined with HMBC and HSQC analysis (see Figures S13 and S17), it can be confirmed that the signal located at δ_C 72.81, 73.48, and 79.80 ppm belong to C-25, C-20, and C-24, respectively. The chemical shifts of C-21 and C-17 in compound **1** occur at δ_C 21.66 and δ_C 52.33 ppm, respectively, which are close to the chemical shifts of C-21 (δ_C 21.5 ppm) and C-17 (δ_C 52.2 ppm) in 20*R*-Rg3.[29] Therefore, it can be inferred that the C-20 in compound **1** is *R*-configuration. The chemical shift of C-21 in compound **1** exhibits a downfield shift from δ_C 13.07 ppm, as observed in ginsenoside Rg5, to δ_C 21.66 ppm. This shift can be attributed to the deshielding effect exerted by the hydroxyl groups attached to C-20. The C-24 of compound **1** is a chiral carbon atom. According to literature,[29] the *R*/*S* configuration of C-24 has little effect on its own chemical shift but has a certain impact on the chemical shifts of C-22, C-25, and C-26, especially on C-22. In the 24*S* configuration, the chemical shift of C-22 is in a relatively high field, while in the 24*R* configuration, the chemical shift of C-22 is in a relatively low field. Both compound **1** and compound **2** have a 20*R* configuration. However, in the comparison of chemical shifts of C-22, it was found that the chemical shift of C-22 in compound **1** (δ_C 140.64) is smaller than that in compound **2** (δ_C 141.05), indicating that the configuration of C-24 in compound **1** may be an *S*-configuration. In order to clarify the configuration of C24 in compound **1**, the CD analysis was conducted by using the Snatzke method.[30] The main principle of the Snatzke method is that chiral 1,2-diols interact with $Mo_2(AcO)_4$ to generate chiral ligands, and five Cotton effects (*I*−*V*) can be observed in the range of 250−650 nm. The CD positive and negative signs of Cotton effects IV and II near 300−310 and 400 nm are determined by the original absolute configuration of the 1,2-diol ligand. In other words, when the

https://doi.org/10.1021/acsomega.5c01444
ACS Omega 2025, 10, 15732−15743

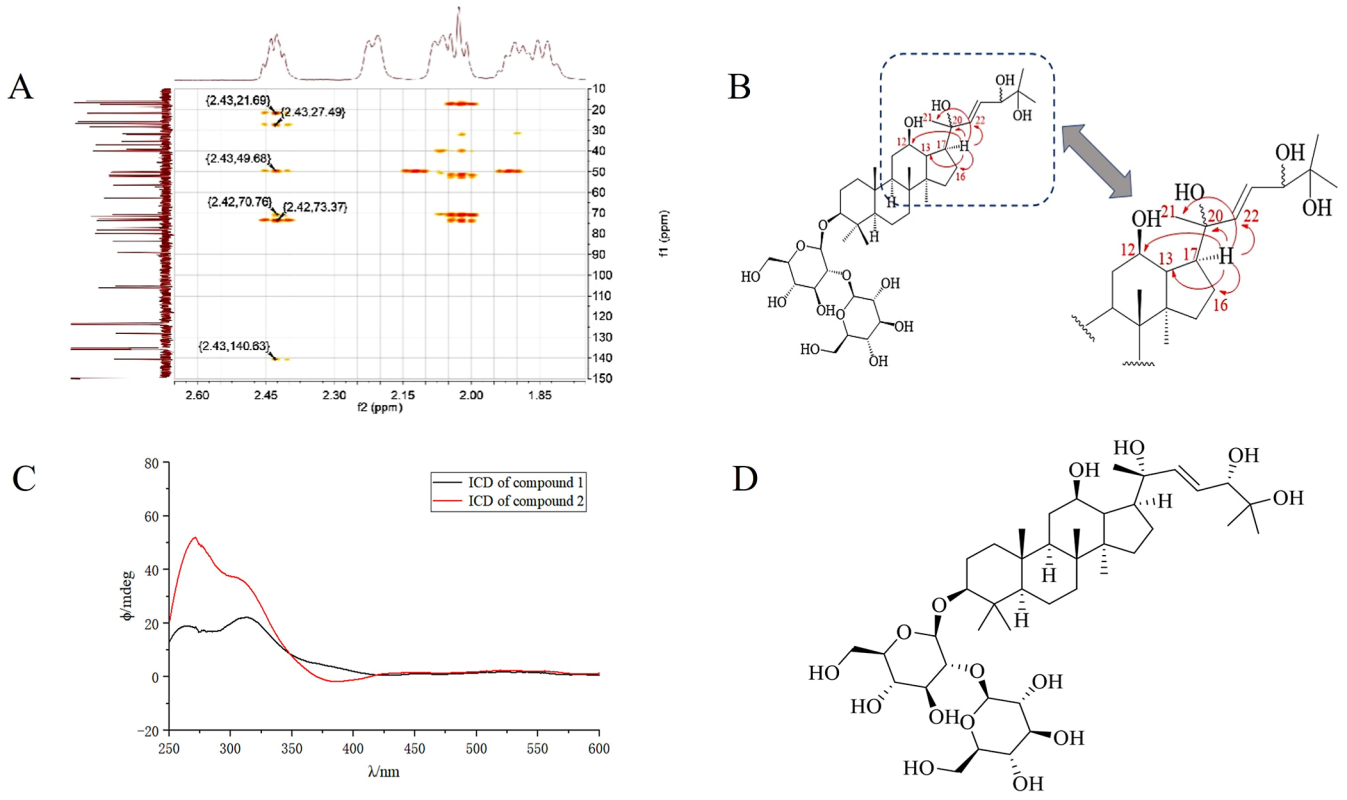

Figure 4. Structure analysis spectrum and structure of compound **1**. (A) Local spectrum of HMBC analysis for compound **1**; (B) schematic diagram of carbon correlation for H-17; (C) $Mo_2(AcO)_4$-induced CD (ICD) spectra of compounds **1** and **2**; and (D) structural schematic diagram of compound **1**.

two C−O bonds within the O−C−C−O moiety of the adjacent diol ligand are oriented with a positive torsional angle, a positive Cotton effect is observed. Conversely, if the torsional angle is negative, a negative Cotton effect is produced.[31−33] In this experiment, as illustrated in Figure 4, the initial step involved the conversion of compound **1** and compound **2** into their respective aglycones utilizing a snail enzyme. Subsequently, the aglycone was reacted with the $Mo_2(AcO)_4$ dimer in a DMSO solvent for a duration of 10 min, resulting in the formation of chiral complexes that exhibited parallel and perpendicular coordination. Following this, the circular dichroism (CD) spectra of the chiral complexes were systematically recorded at 10 min intervals over a period of 30 min to ascertain their stereoisomeric configuration. As shown in Figure 4C, compound **1** exhibits positive Cotton effects IV and II at 311 and 380 nm in the ICD spectrum, while compound **2** exhibits negative Cotton effects at 300 and 385 nm. This indicates that compound **1** exists in the form of the dominant structure 1 in Figure 5; that is, the configuration of C24 in compound **1** is the *S*-configuration. The structure of compound **2** is the dominant structure 2 shown in Figure 5, that is, the configuration of C24 in compound **2** is the *R*-configuration. Compound **1** represents a novel derivative that has not been previously documented in the literature, and its structural configuration is illustrated in Figure 4D.

Compound **2** is a white powder, and based on the $[M + Na]^+$ signal of m/z 839.47367 provided by HR-MS, its molecular formula is speculated to be $C_{42}H_{72}O_{15}$, with a degree of unsaturation of 7. It belongs to a nonenantiomeric stereoisomer with compound **1**. The ^{1}H NMR analysis of compound **2** shows two coupled signals at δ_H 6.36 ppm (1H, d, J = 15.6 Hz) and δ_H 6.45 ppm (1H, dd, J = 6.6, 15.6 Hz). These signals suggest the presence of two hydrogen atoms, each bonded to distinct carbon atoms involved in a double bond within compound **2**. The coupling constant (J) is measured to be 15.6 Hz, which is indicative of an E-configuration for the double bond structure. The singlet signals appearing at δ_H 0.85, 0.94, 1.03, 1.13, 1.32, 1.56, 1.56, and 1.56 ppm belong to methyl hydrogens at positions 19, 30, 18, 29, 28, 21, 26, and 27. In addition, it also contains two signals for the anomeric proton of glucoses, namely, the inner proton appearing at δ_H 4.96 ppm (1H, d, J = 7.8 Hz, H-1′) and the outer proton appearing δ_H 5.40 ppm(1H, d, J = 7.2 Hz, H-1″), indicating that compound **2** contains two β-D-glucopyranoses. ^{13}C NMR shows that compound **2** contains 42 carbons, with a C═C bond located at δ_C 141.05 and δ_C 128.30 ppm, respectively. HMBS analysis shows that the double bond carbon appearing at δ_C 141.05 is related to 17-H (see Figure S14); therefore, the double bond can be attributed to C-22 and C-23. The chemical shifts observed for C-21 (δ_C 21.54) and C-17 (δ_C 52.10) closely resemble those of compound **1**, suggesting that the C-20 position in compound **2** possesses an *R*-configuration. The chemical shift of C-22 in compound **2** is δ_C 141.05, which is greater than the δ_C 140.64 ppm of compound **1**. It closely resembles the compound notoginsenoside SP3, which possesses a 24R configuration as described in ref 29. This indicates that the 24C configuration in compound **2** is also characterized as an R-configuration. The results from the ^{1}H NMR and ^{13}C NMR analyses of compound **2** reveal that its structure contains one fewer double bond and three additional hydroxyl groups on the aliphatic chain in comparison to ginsenoside Rg5. Furthermore, it is classified

https://doi.org/10.1021/acsomega.5c01444
ACS Omega 2025, 10, 15732−15743

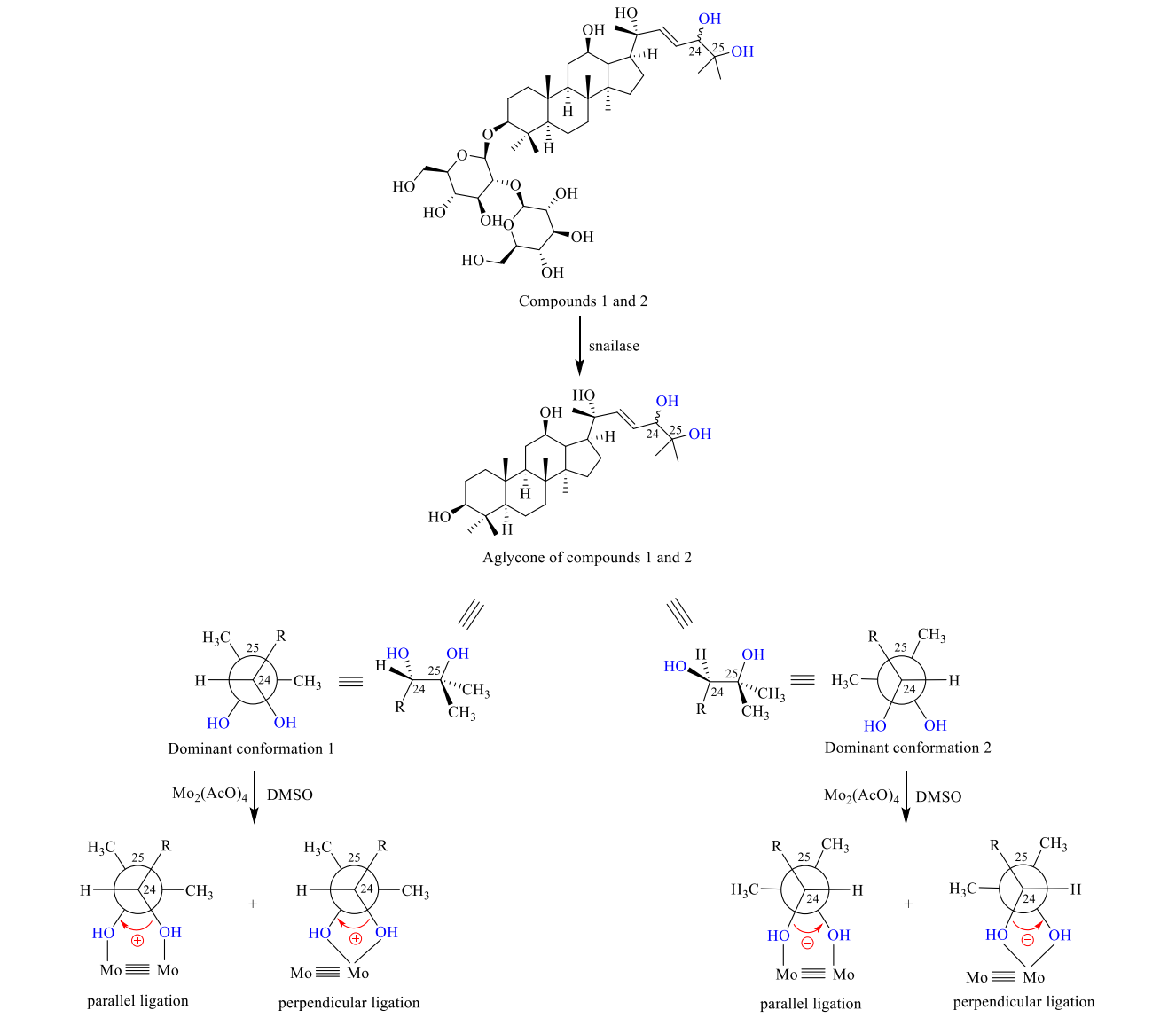

Figure 5. Two most probable conformations for the bidentate ligand of the decomposition product of ginsenoside Rg5 in water onto $[Mo_2(OAc)_4]$ for a negative torsional angle: "parallel" (middle) and "perpendicular" (right).

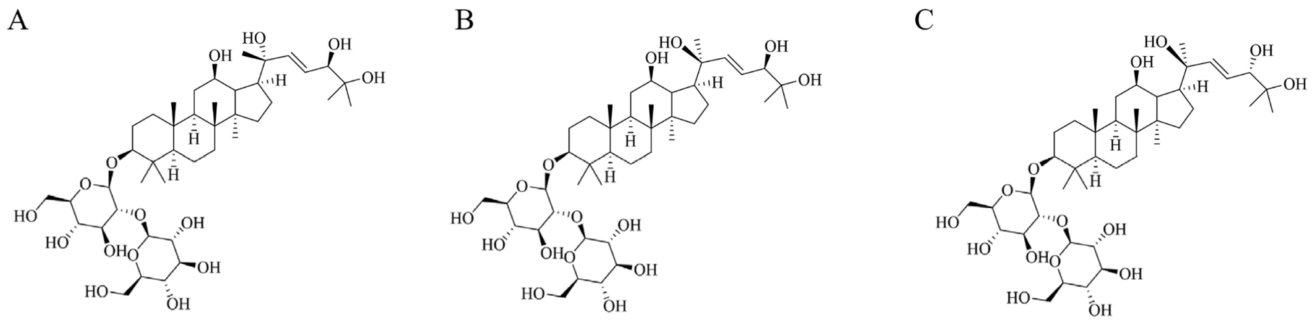

Figure 6. Structural schematic diagram of compound **2** (A), **3** (B), and **4** (C).

as a nonenantiomeric isomer relative to compound **1**. The NMR data of compound **2** is basically consistent with the notoginsenoside SP3 in ref 29, so compound **2** is identified as (3*β*,12*β*,20*R*,22*E*,24*R*)-3,12,20,24,25-pentahydroxydammar-22-en-3-*O*-*β*-D-glucopyranoside (1→2)-*β*-D-glucopyranoside, as shown in Figure 6A.

Compound **3** is a white powder, and based on the $[M + Na]^+$ signal of m/z 839.47492 provided by HR-MS, its molecular formula is speculated to be $C_{42}H_{72}O_{15}$, with a degree of unsaturation of 7. It belongs to a nonenantiomeric stereoisomer with compounds **1**, **2**, and and **4**. The ^1H NMR analysis of compound **3** reveals two coupled signals at δ_H 6.42 ppm (1H, d, J = 15.0 Hz) and δ_H 6.54 ppm (1H, dd, J =

https://doi.org/10.1021/acsomega.5c01444
ACS Omega 2025, 10, 15732−15743

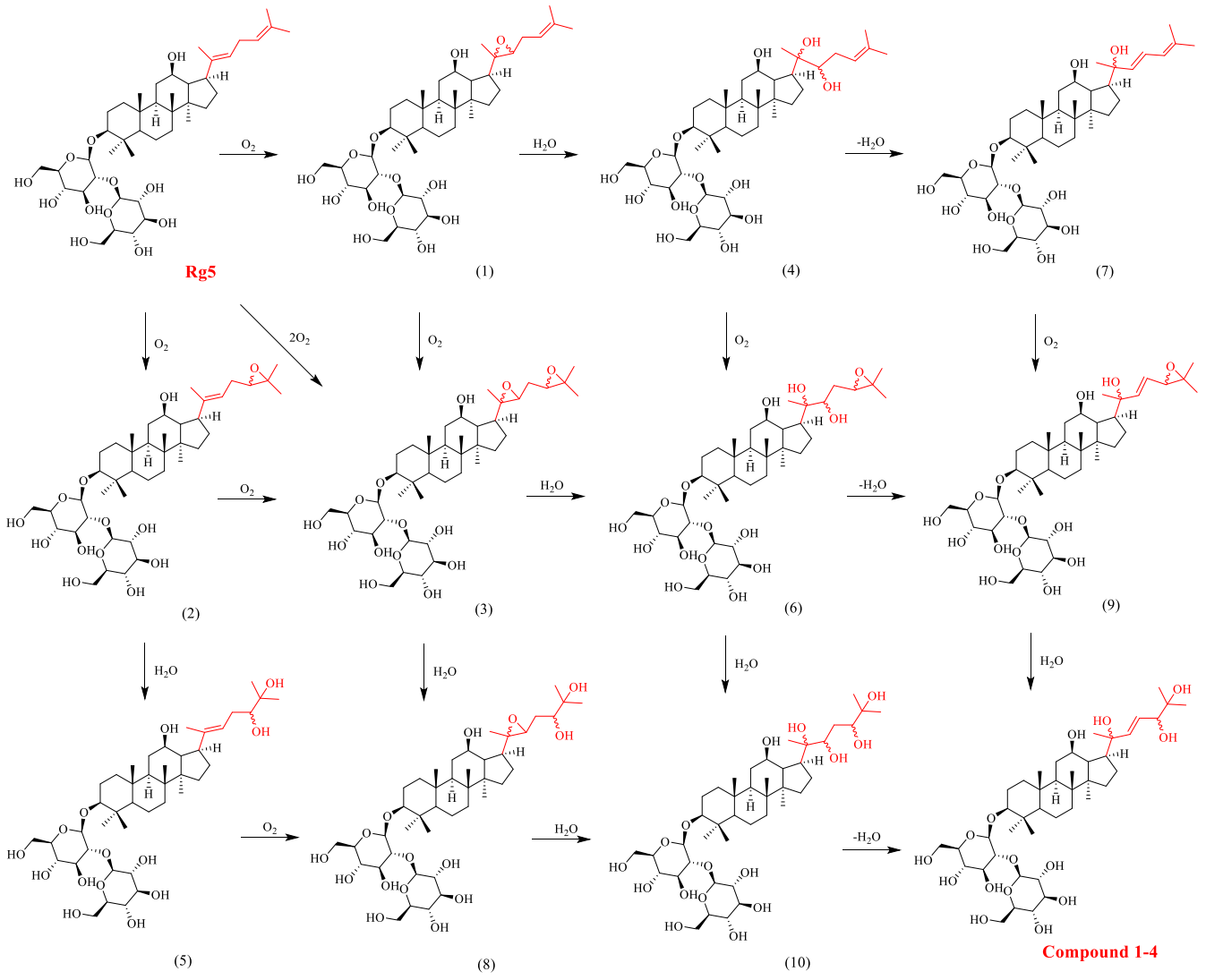

Figure 7. Schematic diagram of possible decomposition pathways of ginsenoside Rg5 in water.

6.6, 15.0 Hz), indicating the presence of two hydrogen atoms associated with distinct double-bonded carbon atoms in compound **3**. The coupling constant (J) is measured to be 15.0 Hz, which suggests that the double bond exhibits an *E*-configuration. The singlet signals appearing at δ_H 0.79, 0.97, 1.01, 1.10, 1.30, 1.56, 1.61, and 1.62 ppm belong to methyl hydrogens at positions 19, 30, 18, 29, 28, 21, 26, and 27. The doublet signals observed at δ_H 4.96 ppm (1H, d, J = 7.8 Hz, H-1′) and δ_H 5.40 ppm (1H, d, J = 7.2 Hz, H-1″) correspond to the inner and outer anomeric protons of glucose units, respectively, suggesting that compound **3** comprises two β-D-glucopyranose moieties. ^{13}C NMR shows that compound **3** has 42 carbon signals and a double bond. The double bond carbon atoms appeared at δ_C 136.40 and δ_C 130.40 ppm, respectively. HMBC analysis shows that the double bond carbon appearing at δ_C 136.40 ppm is related to 17-H (see Figure S15), indicating the double bond can be attributed to C-22 and C-23. In compound **3**, the chemical shifts of C-21 (δ_C 29.30) and C-17 (δ_C 53.75) exhibit a pronounced downfield shift relative to compounds **1** and **2**. Notably, the chemical shift of C-21 demonstrates a substantial downfield displacement of over 7.5 ppm. When considered alongside the ^{13}C NMR data presented in ref 8, it can be conclusively established that the carbon atom at position C-20 in compound **3** possesses an *S*-configuration. The stereochemical configuration of C-24 in compound **3** was investigated by examining the chemical shift of C-22. Given that the configuration of C-21 is identical in both compound **3** and compound **4**, a comparative analysis of the chemical shifts of C-22 in these compounds was conducted. The results indicated that the chemical shift of C-22 in compound **3** is observed at δ_C 136.40, which is downfield relative to the chemical shift in compound **4**, observed at δ_C 136.16. In conjunction with the data presented in ref 29, it is confirmed that the C-24 position in compound **3** exhibits an *R*-configuration. The ^{1}H NMR and ^{13}C NMR analysis results of compound **3** is basically consistent with the notoginsenoside SP2 in ref 29, so compound **3** is identified as (3β,12β,20*S*,22*E*,24*R*)-3,12,20,24,25-pentahydroxydammar-22-en-3-*O*-β-D-glucopyranoside (1→2)-β-D-glucopyranoside, as shown in Figure 6B.

Compound **4** is a white powder, and based on the [M + Na]$^+$ signal of m/z 839.47612 provided by HR-MS, its molecular formula is speculated to be $C_{42}H_{72}O_{15}$, with a degree of unsaturation of 7. It belongs to a nonenantiomeric stereoisomer with compounds **1**, **2**, and and **3**. The ^{1}H NMR analysis of compound **4** reveals two coupled signals at δ_H

https://doi.org/10.1021/acsomega.5c01444
ACS Omega 2025, 10, 15732−15743

6.51 ppm (1H, d, J = 15.6 Hz) and δ_H 6.31 ppm (1H, dd, J = 6.6, 15.6 Hz), indicating the presence of two hydrogen atoms that are associated with two distinct double-bonded carbon atoms within the structure of compound **4**. The coupling constant (J) is measured at 15.6 Hz, which suggests that the double bond exhibits an *E*-configuration. The singlet signals appearing at δ_H 0.81, 0.97, 1.02, 1.10, 1.30, 1.58, 1.58, and 1.60 ppm belong to methyl hydrogens at positions 19, 30, 18, 29, 28, 21, 26, and 27. The doublet signals appearing at δ_H 4.94 ppm(1H, d, J = 7.8 Hz, H-1′) and δ_H 5.38 ppm(1H, d, J = 7.2 Hz, H-1″) belong to the inner and outer anomeric proton of glucoses, indicating that the compound **4** contains two β-D-glucopyranoses. The ^{13}C NMR analysis indicates that compound **4** exhibits 42 distinct carbon signals and contains a double bond. The double bond carbon atoms appeared at δ_C 136.16 and δ_C 130.29 ppm, respectively. HMBC analysis indicates that the carbon associated with the double bond at δ_C 136.16 ppm is correlated with 17-H (refer to Figure S16), suggesting that the double bond can be ascribed to the carbon atoms C-22 and C-23. The chemical shifts of C-21 (δ_C 28.82) and C-17 (δ_C 53.69) in compound **4** move significantly toward the lower field compared to compounds **1** and **2**; especially, the chemical shift of C-21 moves more than 7 ppm toward the lower field. Referring to the ^{13}C NMR data in ref 8, the *S*-configuration of C-20 in compound **4** is confirmed. In addition, it was found that the chemical shift of C-22 in compound **4** appeared at δ_C 136.16, which is higher field than that in compound **3** (δ_C 136.40). Combined with the data from ref 29, it can be confirmed that C-24 in compound **4** has an *S*-configuration. The ^{1}H NMR and ^{13}C NMR analysis results of compound **4** are basically consistent with notoginsenoside SP1 in ref 29. Therefore, compound **4** is identified as (3β,12β,20*S*,22*E*,24*S*)-3,12,20,24,25-pentahydroxydammar-22-en-3-*O*-β-D-glucopyranoside (1→2)-β-D-glucopyranoside, as shown in Figure 6C.

The structure of the decomposition products **1**−**4** of ginsenoside Rg5 in water only changes on the aliphatic chain connected to C17 compared to ginsenoside Rg5. Both molecular formulas of the decomposition products **1**−**4** are $C_{42}H_{72}O_{15}$, which contains one fewer C═C bond and three additional hydroxyl groups in comparison to ginsenoside Rg5. This suggests that the decomposition products of ginsenoside Rg5 in aqueous environments are not produced through the direct hydration of the two C═C double bonds present in the aliphatic chain. Instead, it is probable that these products arise from the oxidation of the C═C double bonds to form epoxy compounds through the action of oxygen, followed by subsequent hydrolysis and dehydration. This implies that dissolved oxygen in water may play a significant role in the decomposition process of Rg5. Considering the absence of the C═C double bonds between C20−C22 and C24−C25 in decomposition products 1−4, along with the emergence of a new C═C double bond between C22 and C23 and the introduction of three hydroxyl groups at C20, C24, and C25, a plausible decomposition pathway for ginsenoside Rg5 can be inferred (see Figure 7).

As shown in Figure 7, the decomposition process of ginsenoside Rg5 is accompanied by reactions such as oxidation, hydrolysis, and dehydration. The first step of decomposition is oxidation by oxygen, and theoretically, it can be oxidized into compounds (**1**), (**2**), or (**3**). There is also a carbon−carbon double bond on the aliphatic chain of ginsenoside Rg3 at positions C24−25, but its stability is much higher than that of Rg5 in the same water environment (see Figure S21). This indicates that the C24−C25 double bond is relatively stable to oxygen, so it can be inferred that the main product of the first step oxidation of ginsenoside Rg5 is not compound (**2**) and (**3**), but compound (**1**). In order to further clarify the possible decomposition pathway of ginsenoside Rg5, HR-MS analysis was performed on a small amount of two monomer compounds 5 and 6 obtained during the separation of ginsenoside Rg5's decomposition products compounds **1**−**4**. The analysis results showed $[M + Na]^+$ion signals at m/z 839.47612 and 821.46519, respectively (see Figures S22 and S23), corresponding to molecular formulas $C_{42}H_{72}O_{15}$ and $C_{42}H_{70}O_{14}$. The molecular formula of compound **5** ($C_{42}H_{72}O_{15}$) is the same as that of compounds (**6**) and (**8**), while the molecular formula of compound **6** ($C_{42}H_{70}O_{14}$) is the same as that of compounds (**3**) and (**9**) in Figure 7, indicating that compounds **5** and **6** are intermediate products of the producing final decomposition products **1**−**4** of ginsenoside Rg5. Considering that the main decomposition pathway of Rg5 is first oxidized by oxygen into compound (**1**), rather than (**2**) and (**3**), and combined with the fact that intermediate product (**9**) can be obtained through dehydration of compound (**6**), it can be inferred that the main decomposition pathway of ginsenoside Rg5 may be Rg5 → (1) → (4) → (6) → (9) → decomposition products **1**−**4**.

In conclusion, ginsenoside Rg5, a decomposition product of the primary ginsenosides found in ginseng roots, has garnered significant attention owing to its notable biological activities, including anticancer properties, immune enhancement, anti-inflammatory effects, and memory improvement, among others. Its diverse pharmacological activities have been the subject of extensive research. Despite the extensive research on the pharmacological activity of ginsenoside Rg5, there has been limited focus on its stability. The stability of pharmaceutical compounds is critical as it significantly influences their efficacy and safety. A comprehensive understanding of the factors contributing to drug instability is essential for preventing structural alterations, thereby enhancing the safety and effectiveness of medications. Furthermore, this study is invaluable for establishing guidelines regarding the shelf life, storage, and transportation of pharmaceutical products. Water is ubiquitously present in natural environments, including oceans, rivers, lakes, swamps, the atmosphere, and soil, all of which contain substantial quantities of water. Furthermore, water constitutes the predominant component in the majority of living organisms. In this study, we investigated the stability of ginsenoside Rg5 in aqueous environments, isolated the primary decomposition products, conducted structural characterization, and proposed potential decomposition pathways based on the structural features of the decomposition products. The structural characterization of the decomposition products of ginsenoside Rg5 in aqueous solution showed that compounds **1**−**4** were (3β,12β,20*R*,22*E*,24*S*)-3,12,20,24,25-pentahydroxydammar-22-en-3-*O*-β-D-glucopyranoside (1→2)-β-D-glucopyranoside; (3β,12β,20*R*,22*E*,24*R*)-3,12,20,24,25-pentahydroxydammar-22-en-3-*O*-β-D-glucopyranoside (1→2)-β-D-glucopyranoside; (3β,12β,20*S*,22*E*,24*R*)-3,12,20,24,25-pentahydroxydammar-22-en-3-*O*-β-D-glucopyranoside (1→2)-β-D-glucopyranoside; and (3β,12β,20*S*,22*E*,24*S*)-3,12,20,24,25-pentahydroxydammar-22-en-3-*O*-β-D-glucopyranoside (1→2)-β-D-glucopyranoside. Among these, compound **1** is a novel derivative that has not been previously reported in the literature. The structure of the decomposition products of

https://doi.org/10.1021/acsomega.5c01444
ACS Omega 2025, 10, 15732−15743

Rg5 suggests that the decomposition product of ginsenoside Rg5 is formed by the oxidation of ginsenoside Rg5 by dissolved oxygen in aqueous environment, leading to the formation of epoxide. The intermediate products are further decomposed into compounds **1**−**4** through a series of reactions such as hydrolysis of epoxide, oxidation of double bond, dehydration of alcohol, and hydrolysis of another epoxide. Obviously, dissolved oxygen in aqueous and humid environments is a primary factor contributing to the instability of ginsenoside Rg5. This underscores the importance of isolating ginsenoside Rg5 from water and air to preserve its stability. While ginsenoside Rg5 is recognized as a promising natural medicine, its limited stability in water adversely impacts its pharmacological efficacy, particularly in relation to the anticancer activity of its decomposition products, which is significantly diminished (see Figures S24 and S25). Additionally, this instability poses challenges for storage. Comprehending the primary factors contributing to the instability of ginsenoside Rg5 in aqueous environments is crucial for enhancing its stability and facilitating its development and application in natural medicine.

EXPERIMENTAL SECTION

General Experimental Procedures. HPLC analysis was performed on a Dalian Elite P230 liquid chromatograph with reverse phase chromatography column (5 μm, 250 × 4.6 mm), P230P high-pressure constant flow pump, UV230$^+$ ultraviolet−visible detector, and EC-2000 LU workstation. The rotary evaporator (Re-2000A, Shanghai Yarong) and high-speed centrifuge (H2050R, Hunan Xiangyi) were used for concentration and centrifugation. The TS200B desktop constant temperature oscillator was used for the decomposition of ginsenoside Rg5 in water. The GX281 preparative HPLC (Gilson Technology Co., Ltd.) was used for the separation of the decomposition products of ginsenoside Rg5. The 1D NMR and 2D NMR (^{1}H−^{13}C HSQC and ^{1}H−^{13}C HMBC) spectra were obtained on a Bruker 600 MHz instrument. High-resolution mass spectroscopy (HR-MS) was performed on an Agilent 7250& JEOL-JMS-T100LP AccuTOF. Induced circular dichroism (ICD) was detected with a Chirascan circular dichroism spectrograph (Applied Photophysics Ltd., England). Rg5, 98% purity, was purchased from the Shanghai Yuanye Biotechnology Co., Ltd. (China). HPLC-grade acetonitrile and methanol were purchased from the Tedia Company (U.S.) and Tianjin Damao Chemical Reagent Factory (China). Snailase was purchased from Beijing Biodee Biotechnology Co., Ltd. (China). MIC GEL CHP20/P120 was purchased from Beijing Green Herbs Biotechnology Co., Ltd. (China). Purified water was purchased from Hangzhou Wahaha Group Co., Ltd. (China). Silica gel 60 F254 thin-layer plate (TLC) was purchased from Merck (Germany).

Preparation of Stock Solution for Ginsenoside Rg5. Precisely weighed ginsenoside Rg5 (12.5 mg) was dissolved in HPLC-grade methanol and diluted to 25 mL in a volumetric flask to prepare a stock solution, which was subsequently stored at 4 °C for future use. For stability experiments, the stock solution was concentrated to dryness using a rotary evaporator at 30 °C. A specific volume of pure water was then added to obtain a Rg5 aqueous solution with a concentration of 0.1 mg/mL, and its stability was evaluated.

Stability Analysis of Ginsenoside Rg5 in Water. Fifteen samples of ginsenoside Rg5 aqueous solution were subjected to agitation in a desktop shaker oscillator at 100 rpm (rpm) for a duration of 2−10 days at room temperature. Every 2 days, three samples should be collected for parallel experimentation. These samples are to be evaporated to dryness and then filtered using a 0.22 μm filter. Subsequently, the residual concentration of Rg5 should be analyzed using high-performance liquid chromatography (HPLC).

Separation and Characterization of Decomposition Products of Rg5 in Water. Ginsenoside Rg5 (375 mg) was dissolved in purified water (500 mL) and subjected to agitation using a desktop shaker oscillator at 25 °C for a duration of 10 days. Subsequently, the solution was maintained at 45 °C for an additional 10 days to facilitate accelerated decomposition. After the introduction of ethanol to the reaction mixture, water was removed using azeotropic distillation. Subsequently, the main decomposition products were isolated through preparative liquid chromatography, leading to the acquisition of compounds **1**−**4**. These compounds were then characterized using HR-MS, 1D-NMR, 2D-NMR, and ICD.

Stereoscopic Characterization of Decomposition Products. The hydrolysis of the glycosidic bond in the compound was conducted as described in the referenced study, and this process does not alter the stereoconfiguration of these compounds.[30] Compound **1** and compound **2** (each 11 mg) in HAc-NaAc buffer (pH 5.5, 11 mL) were hydrolyzed with snailase (11 mg) at 50 °C for 36 h. The reaction mixture was centrifuged, and the solid portion was washed repeatedly with distilled water three times. Then, the mixture was subjected to MIC GEL CHP20/P120 column and eluted with 10% MeOH, 70% MeOH, and 100% MeOH, respectively. The 100% MeOH fraction was evaporated to dryness at 30 °C and yielded 5.8 mg of aglycones compound **1** and 4.2 mg of compound **2**. $Mo_2(AcO)_4$-induced circular dichroism (ICD analysis was conducted according to the methods in the literature.[29] 0.7 mg of $Mo_2(AcO)_4$ was dissolved in 1 mL of DMSO, and then were added 0.5 mg of aglycones compound **1** and aglycones compound **2**. Following a 10 min mixing period, ICD analysis was promptly conducted to characterize the stereoconfiguration of adjacent diols within the saponin fatty chain.[29]

Separation Method for the Decomposition Products of Ginsenoside Rg5 in Water. The decomposition products of ginsenoside Rg5 in water were separated by GX281 preparative HPLC. The preparative HPLC conditions were as follows: chromatography column, Waters C18 column (210 mm × 19 mm, 5 μm); UV detector; detection wavelength, 203 nm; mobile phase: (A) 0.1% formic acid aqueous solution, (B) acetonitrile, water; gradient elution program: 0−30 min, 30−60%.

HPLC Analysis. Column: RESTEK Pinnacle II C18 column (250 mm × 4.6 mm, 5 μm), UV detector; detection wavelength, 203 nm; injection volume, 20 μL; column temperature, 35 °C; volume flow, 1 mL/min. Mobile phase: (A) acetonitrile, (B) purified water; gradient elution program: 0−22 min, 28−90% A; 22−27 min, 90% A. Column: Welch Unmite C18 column (4.6 mm × 150 mm, 5 μm), UV detector; detection wavelength, 203 nm; volume flow, 1 mL/min. Mobile phase: A: 10 mmol/L NH_4HCO_3 in water, B: CH_3CN. gradient elution program: 0−3 min, 5% B; 3−8 min, 5−95% B; 8−12 min, 95% B.

TLC Analysis. Ginsenosides were dissolved in methanol and subsequently applied to thin-layer chromatography (TLC) plates utilizing glass capillaries. A mixed solvent system comprising chloroform, methanol, and water in a volumetric

https://doi.org/10.1021/acsomega.5c01444
ACS Omega 2025, 10, 15732−15743

ratio of 65:35:10 (v/v/v) was employed as the developing agent. Following solvent application, the sample was subjected to blow drying. Subsequently, a 10% aqueous sulfuric acid solution was sprayed onto the sample, which was then heated at 110 °C to facilitate color development.

■ ASSOCIATED CONTENT

Supporting Information

The Supporting Information is available free of charge at https://pubs.acs.org/doi/10.1021/acsomega.5c01444.

HR-MS and 1D and 2D NMR spectra for compounds **1**−**4** (PDF)

■ AUTHOR INFORMATION

Corresponding Authors

Leqin Cheng − *School of Chemistry and Pharmaceutical Engineering, Jilin Institute of Chemical Technology, Jilin 132022, China*; Email: chengleqin@126.com

Yuewei Zhang − *School of Chemistry and Pharmaceutical Engineering, Jilin Institute of Chemical Technology, Jilin 132022, China*; orcid.org/0000-0001-6696-0336; Email: zhangyueweichem@163.com

Authors

Anqi Ye − *School of Chemistry and Pharmaceutical Engineering, Jilin Institute of Chemical Technology, Jilin 132022, China*

Yunqi Tao − *School of Chemistry and Pharmaceutical Engineering, Jilin Institute of Chemical Technology, Jilin 132022, China*

Complete contact information is available at: https://pubs.acs.org/10.1021/acsomega.5c01444

Notes

The authors declare no competing financial interest.

■ ACKNOWLEDGMENTS

This study was financially supported by Jilin Provincial Science and Technology Development Program (YYZX202009). Figure 1 was created with BioRender.com.

■ REFERENCES

(1) Zhao, J.; Su, C.; Yang, C.; Liu, M.; Tang, L.; Su, W.; Liu, Z. Determination of ginsenosides Rb1, Rb2, and Rb3 in rat plasma by a rapid and sensitive liquid chromatography tandem mass spectrometry method: Application in a pharmacokinetic study. *J. Pharm. Biomed. Anal.* **2012**, *64*−*65*, 94−97.

(2) Chu, Y.; Zhang, H.-c.; Li, S.-m.; Wang, J.-m.; Wang, X.-y.; Li, W.; Zhang, L.-l.; Ma, X.-h.; Zhou, S.-p.; Zhu, Y.-h.; et al. Determination of ginsenoside Rc in rat plasma by LC−MS/MS and its application to a pharmacokinetic study. *J. Chromatogr. B* **2013**, *919*−*920*, 75−78.

(3) Han, M. J.; Kim, D.-H. Effects of Red and Fermented Ginseng and Ginsenosides on Allergic Disorders. *Biomolecules* **2020**, *10* (4), 634.

(4) Fan, W.; Fan, L.; Wang, Z.; Mei, Y.; Liu, L.; Li, L.; Yang, L.; Wang, Z. Rare ginsenosides: A unique perspective of ginseng research. *J. Adv. Res.* **2024**, *66*, 303−328.

(5) Zhang, H.; Park, S.; Huang, H.; Kim, E.; Yi, J.; Choi, S. K.; Ryoo, Z.; Kim, M. Anticancer effects and potential mechanisms of ginsenoside Rh2 in various cancer types (Review). *Oncol. Rep.* **2021**, *45* (4), 33.

(6) Park, E.-H.; Kim, Y.-J.; Yamabe, N.; Park, S.-H.; Kim, H.-k.; Jang, H.-J.; Kim, J. H.; Cheon, G. J.; Ham, J.; Kang, K. S. Stereospecific anticancer effects of ginsenoside Rg3 epimers isolated from heat-processed American ginseng on human gastric cancer cell. *J. Ginseng Res.* **2014**, *38* (1), 22−27.

(7) Kim, S. I.; Park, J. H.; Ryu, J.-H.; Park, J. D.; Lee, Y. H.; Park, J.-H.; Kim, T.-H.; Kim, J. M.; Baek, N.-I. Ginsenoside Rg5, a genuine dammarane glycoside from Korean red ginseng. *Arch. Pharmacal Res.* **1996**, *19* (6), 551−553.

(8) Kim, S.-J.; Kim, A. K. Anti-breast cancer activity of Fine Black ginseng (Panax ginseng Meyer) and ginsenoside Rg5. *J. Ginseng Res.* **2015**, *39* (2), 125−134.

(9) Jo, S. K.; Kim, I. S.; Yoon, K. S.; Yoon, H. H.; Yoo, H. H. Preparation of ginsenosides Rg3, Rk1, and Rg5-selectively enriched ginsengs by a simple steaming process. *Eur. Food Res. Technol.* **2015**, *240* (1), 251−256.

(10) Guo, D.-d.; Cheng, L.-q.; Zhang, Y.-w.; Zheng, H.-c.; Ma, H.-y.; Li, L. An improved method for the preparation of Ginsenoside Rg5 from ginseng fibrous root powder. *Heliyon* **2019**, *5* (10), No. e02694.

(11) Chen, J.; Li, M.; Huo, X.; Li, Z.; Qu, D.; Sha, J.; Sun, Y. A Novel Process for One-Step Separation and Cyclodextrin Inclusion of Ginsenoside Rg5 from Ginseng Stem−Leaf Saponins (GSLS): Preparation, Characterization, and Evaluation of Storage Stability and Bioactivity. *Foods* **2023**, *12* (12), 2349.

(12) Le-qin, C.; An-qi, Y.; Hao-ran, Z.; Yue-wei, Z.; Ling, L. An efficient synthesis of ginsenoside Rg5 via conversion of PPD type saponins: Unusual application of 4A molecular sieves. *Nat. Prod. Commun.* **2021**, *16* (4), 1934578X211007637.

(13) Bae, E.-A.; Han, M. J.; Choo, M.-K.; Park, S.-Y.; Kim, D.-H. Metabolism of 20(S)-and 20(R)-ginsenoside Rg3 by human intestinal bacteria and its relation to in vitro biological activities. *Biol. Pharm. Bull.* **2002**, *25* (1), 58−63.

(14) Yu, H.; Wang, Y.; Liu, C.; Yang, J.; Xu, L.; Li, G.; Song, J.; Jin, F. Conversion of ginsenoside Rb1 into six types of highly bioactive ginsenoside Rg3 and its derivatives by $FeCl_3$ catalysis. *Chem. Pharm. Bull.* **2018**, *66* (9), 901−906.

(15) Liu, Y.; Fan, D. The preparation of ginsenoside Rg5, its antitumor activity against breast cancer cells and its targeting of PI3K. *Nutrients* **2020**, *12* (1), 246.

(16) Chen, C.; Lv, Q.; Li, Y.; Jin, Y.-H. The anti-tumor effect and underlying apoptotic mechanism of ginsenoside Rk1 and Rg5 in human liver cancer cells. *Molecules* **2021**, *26* (13), 3926.

(17) Zhang, D.; Wang, A.; Feng, J.; Zhang, Q.; Liu, L.; Ren, H. Ginsenoside Rg5 induces apoptosis in human esophageal cancer cells through the phosphoinositide-3 kinase/protein kinase B signaling pathway. *Mol. Med. Rep.* **2019**, *19* (5), 4019−4026.

(18) Feng, S.-L.; Luo, H.-B.; Cai, L.; Zhang, J.; Wang, D.; Chen, Y.-J.; Zhan, H.-X.; Jiang, Z.-H.; Xie, Y. Ginsenoside Rg5 overcomes chemotherapeutic multidrug resistance mediated by ABCB1 transporter: in vitro and in vivo study. *J. Ginseng Res.* **2020**, *44* (2), 247−257.

(19) Xiao, N.; Lou, M.-D.; Lu, Y.-T.; Yang, L.-L.; Liu, Q.; Liu, B.; Qi, L.-W.; Li, P. Ginsenoside Rg5 attenuates hepatic glucagon response via suppression of succinate-associated HIF-1α induction in HFD-fed mice. *Diabetologia* **2017**, *60*, 1084−1093.

(20) Kim, T.-W.; Joh, E.-H.; Kim, B.; Kim, D.-H. Ginsenoside Rg5 ameliorates lung inflammation in mice by inhibiting the binding of LPS to toll-like receptor-4 on macrophages. *Int. Immunopharmacol.* **2012**, *12* (1), 110−116.

(21) Kim, E.-J.; Jung, I.-H.; Van Le, T. K.; Jeong, J.-J.; Kim, N.-J.; Kim, D.-H. Ginsenosides Rg5 and Rh3 protect scopolamine-induced memory deficits in mice. *J. Ethnopharmacol.* **2013**, *146* (1), 294−299.

(22) Panossian, A.; Abdelfatah, S.; Efferth, T. Network pharmacology of red ginseng (part I): Effects of ginsenoside Rg5 at physiological and sub-physiological concentrations. *Pharmaceuticals* **2021**, *14* (10), 999.

(23) Kim, W. Y.; Kim, J. M.; Han, S. B.; Lee, S. K.; Kim, N. D.; Park, M. K.; Kim, C. K.; Park, J. H. Steaming of ginseng at high temperature enhances biological activity. *J. Nat. Prod.* **2000**, *63* (12), 1702−1704.

(24) Song, L. H.; Zhang, R.; Xu, T. Y.; Yu, P. Effects of different drying methods and temperatures on the content of chemical

components and antioxidant activity of Ginseng decoction pieces. *Lishizhen Med. Mater. Med. Res.* **2023**, *34* (10), 2412−2418.
(25) Zhu, W.; Zhang, L.; Fang, J.; Zhang, H. Study on the stability of ginsenoside compound-K hydrates. *Chin. J. Antibiot.* **2022**, *47* (04), 366−369.
(26) Kwok, K.; Mauer, L. J.; Taylor, L. S. Kinetics of moisture-induced hydrolysis in powder blends stored at and below the deliquescence relative humidity: investigation of sucrose-citric acid mixtures. *J. Agric. Food Chem.* **2010**, *58* (22), 11716−11724.
(27) Samuelsen, L.; Holm, R.; Lathuile, A.; Schönbeck, C. Buffer solutions in drug formulation and processing: How pK(a) values depend on temperature, pressure and ionic strength. *Int. J. Pharm.* **2019**, *560*, 357−364.
(28) Fagan, A.; Bateman, L. M.; O'Shea, J. P.; Crean, A. M. Kinetics of human insulin degradation in the solid-state: An investigation of the effects of temperature and humidity. *J. Pharm. Sci.* **2025**, *114* (2), 1368−1375.
(29) Gu, C.-Z.; Lv, J.-J.; Zhang, X.-X.; Qiao, Y.-J.; Yan, H.; Li, Y.; Wang, D.; Zhu, H.-T.; Luo, H.-R.; Yang, C.-R.; et al. Triterpenoids with promoting effects on the differentiation of PC12 cells from the steamed roots of Panax notoginseng. *J. Nat. Prod.* **2015**, *78* (8), 1829−1840.
(30) Yu ZhaoHui, Y. Z.; Liu QiYuan, L. Q.; Cui Li, C. L.; Jia XiaoBin, J. X.; Jin Xin, J. X. Study on the preparation of rare ginsenoside Compound K by enzymolysis of ginsenoside Rb1 with snailase. *China J. Tradit. Chin. Med. Pharm.* **2015**, *30* (02), 412−416.
(31) Di Bari, L.; Pescitelli, G.; Pratelli, C.; Pini, D.; Salvadori, P. Determination of absolute configuration of acyclic 1,2-diols with $Mo_2(OAc)_4$. 1. Snatzke's method revisited. *J. Org. Chem.* **2001**, *66* (14), 4819−4825.
(32) Frelek, J.; Ikekawa, N.; Takatsuto, S.; Snatzke, G. Application of $[Mo_2(OAc)_4]$ for determination of absolute configuration of brassinosteroid vic-diols by circular dichroism. *Chirality* **1997**, *9* (5−6), 578−582.
(33) Liu, J.; Du, D.; Si, Y.; Lü, H.; Wu, X.; Li, Y.; Liu, Y.; Yu, S. Application of Dimolybdenum Reagent Mo_2 $(OAc)_4$ for Determination of the Ab-solute Configurations of vic-Diols. *China J. Org. Chem.* **2010**, *30* (09), 1270−1278.

https://doi.org/10.1021/acsomega.5c01444
ACS Omega 2025, 10, 15732−15743